ELSEVIER

Biochimica et Biophysica Acta 1363 (1998) 187–198

BIOCHIMICA ET BIOPHYSICA ACTA
BBA

Determination of distances from tyrosine D to Q_A and chlorophyll$_Z$ in photosystem II studied by '2 + 1' pulsed EPR

Kazuhito Shigemori [a], Hideyuki Hara [a], Asako Kawamori [a,*], Kozo Akabori [b]

[a] *Faculty of Science, Kwansei Gakuin University, Uegahara 1-1-155, Nishinomiya 662, Japan*
[b] *Faculty of Integrated Arts and Sciences, Hiroshima University, Higashi-Hirosima 739, Japan*

Received 12 September 1997; accepted 5 December 1997

Abstract

A '2 + 1' pulse sequence electron spin echo (ESE) method was applied to measure the dipole interactions between the tyrosine Y_D^+ and Q_A^- in Photosystem II (PS II). In a CN^--treated PS II, Q_A^- EPR signal was observed at $g = 2.0045$ position, because the non-heme Fe(II) was converted into a low-spin ($S = 0$) state. The radical pair of $Y_D^+Q_A^-$ was trapped by illumination for 8 min at 273 K, followed by dark adaptation for 3 min and freezing into 77 K. By using a proton matrix ENDOR, these trapped radicals were confirmed to be Y_D^+ and Q_A^-, respectively. The distance between the radical pair was estimated from the dipole interaction constant fitted to the observed '2 + 1' ESE time profile. The distance of Y_D^+–Q_A^- is determined to be 38.8 ± 1.1 Å. The magnetic dipole interaction between Y_D^+ and Chl_Z^+ was determined in a Tris-treated PS II in which Chl_Z^+ was generated by illumination at 200 K for 10 min. The Y_D^+–Chl_Z^+ distance was estimated to be 29.4 ± 0.5 Å. © 1998 Elsevier Science B.V.

Keywords: Photosystem II; Tyrosine D; Q_A; Chlorophyll$_Z$; Electron spin echo

1. Introduction

In higher plants Photosystem II (PS II) is composed of multi-subunit integral and extrinsic membrane protein complexes. In the D1 and D2 subunits, almost all electron transfer components of PS II, the primary electron donor P680, an intermediate electron acceptor pheophytin, the primary electron acceptor quinone Q_A, the secondary electron acceptor quinone Q_B, and the tyrosine donor Y_Z (tyrosine-161 in D1 subunit of PS II) are included [1,2]. Besides, Y_D (another redox active tyrosine in D2 subunit) takes part in charge recombinations with the redox components in the oxygen evolving complexes (OEC) [1] or Q_A^- [3].

Abbreviations: PS II, Photosystem II; Y_D, tyrosine-161 in D2 subunit of PS II; Y_Z, tyrosine-161 in D1 subunit of PS II; Q_A, the primary electron acceptor in PS II; P680, the primary electron donor in PS II; Chl$_Z$, a donor chlorophyll to P680; Cyt, cytochrome; Tricine, *N*-Tris(hydroxymethyl)methylglycine; Mops, 4-morpholinopropanesulfonic acid; hfi, hyperfine interaction; m.w., micro wave; EPR, electron paramagnetic resonance; ESE, electron spin echo; ELDOR, electron–electron double resonance; ENDOR, electron–nuclear double resonance; rf, radio frequency; CW, continuous wave

* Corresponding author. Fax: +81-798-51-0914; E-mail: kawamori@kwansei.ac.jp

PII S0005-2728(97)00100-X

In the normal electron transfer reaction, a photooxidized P680 is reduced by Y_Z and then the oxidized Y_Z^+ is reduced by the Mn-cluster in OEC [1,2]. In a Mn-depleted PS II, Y_Z^+ recombines with the reduced Q_A^- [4,5]. Y_Z plays an important role as an intermediate in this reaction. Although Y_Z and Y_D are suggested to be at symmetric positions of P680 [6,7], Y_D dose not play a definite role in the major electron transfer reaction. Therefore, elucidation of the structure of Photosystem II is essential for better understanding of these heterogeneous electron transfer mechanism.

The structures of the photosynthetic reaction center of the purple non-sulfur bacteria *Rhodopseudomonas viridis* [8] and *Rhodobacter sphaeroides* [9] were analyzed by X-ray studies. The similarities between the amino acid sequences of the L and M subunits of the bacterial reaction center and the D1 and D2 subunits of PS II have provided some insight into the structure of the D1/D2 complex [10,11]. Based on the structures of the bacterial reaction centers, computer simulations on the structure of the PS II have been carried out [6,12,13]. However, the structure of PS II has not yet been clarified, because crystallization of PS II reaction center suitable for X-ray analysis has not yet been successful.

Instead of X-ray analysis, the distances between several paired paramagnetic centers in PS II have been determined by EPR studies in order to determine the relative position of the redox-active components in PS II reaction center. The distance between P680 and the Mn-cluster in OEC was estimated to be 21–26 Å by a time resolved EPR measurement of the light induced $P680^+$ [14]. The distance between Y_D and the non-heme Fe(II) in PS II was estimated to be 37 ± 5 Å by using the EPR measurement of the spin-lattice relaxation time [15]. The location of Y_D was estimated to be 27 Å and 26 Å from the inner and outer thylakoid surfaces, respectively [16]. The distance between Y_Z and the non-heme Fe(II) was also estimated to be 37 ± 5 Å by using an EPR measurement of spin-lattice relaxation times and symmetric locations of Y_D and Y_Z to the non-heme Fe(II) were suggested [17]. Furthermore, the location of Chl_Z in PS II was estimated to be 27 Å from the inner and outer thylakoid surfaces, respectively, and 39.5 ± 2.5 Å from the non-heme Fe(II) by using the same method [18]. The location of the Mn-cluster relative to Y_Z has been suggested from spin-lattice relaxation rate in Ca-depleted PS II measured by the pulsed EPR to be 15–20 Å [19]. On the other hand, it is suggested based on the pulsed ENDOR and a hydrogen abstraction model to be 4.5 Å [20,21]. A recent pulsed ELDOR method determined the distance of the manganese paramagnetic center in the S_2-state from Y_D to be 27 ± 0.2 Å very accurately [22]. The distance between Y_D and Y_Z was estimated to be 29–30 Å by using the '2 + 1' ESE method [23].

The '2 + 1' pulse sequence electron spin echo method is a special case of general ELDOR methods. By using a '2 + 1' ESE method, we can selectively detect the magnetic dipole interaction between radicals and can estimate the distance between the radicals. As other methods cannot selectively detect the magnetic dipole interaction, the values obtained by a '2 + 1' ESE method are most accurate among the values derived by other methods. It employs a sequence of three m.w. pulses with the same carrier frequency and is useful when the EPR transitions of the paramagnetic centers can be efficiently excited by the pulses. This implies that the EPR spectra of studied species have to be reasonably narrow, of the order of $10 \sim 20$ G, and overlapping each other as studied in Refs. [23–25].

EPR signals of Y_D^+ and Y_Z^+ have been studied in detail to elucidate the difference in their microenvironments [26–30]. Both spectra show the almost same hyperfine splitting with the intensity ratio about 1:3:3:1, which has been ascribed to couplings with one of the β-methylene protons and the two equivalent 3,5-ring protons. Although there is a slight difference between both spectra related to the β-methylene orientation [26–29], it is difficult to discriminate the one from the other by a conventional EPR.

Q_A^- EPR signal in oxygen-evolving or Mn-depleted PS II can be observed only below 8 K at $g \approx 1.65$, $g \approx 1.82$, and $g \approx 1.95$ with a broad width caused by a magnetic exchange coupling with non-heme Fe(II), which is in a high-spin $(S = 2)$ state in an ordinary untreated or a Tris-treated PS II [31]. However, in a CN^--treated PS II, incubated at high CN^- concentration and high pH, the non-heme Fe(II) was converted into its low-spin $(S = 0)$ state, because three cyanides bind to the non-heme Fe(II) [32]. Accordingly, a sharp Q_A^- EPR signal, magnetically decoupled from the non-heme Fe(II), can be observed at $g = 2.0045$ with $\Delta H \approx 9$ G [32]. In the CN^--treated PS II, isolated from the cyanobacterium *Synechocystis* sp. PCC 6803, site-directed

mutagenesis of Y_D residue to phenylalanine, the radical pair of $Y_Z^+Q_A^-$ was trapped by freezing under illumination [17]. In a spinach CN^--treated PS II, if the radical pair of $Y_Z^+Q_A^-$ or $Y_D^+Q_A^-$ can be trapped separately under controlled illumination condition, these radical pairs will satisfy the condition applicable to a '2 + 1' ESE method.

Chl_Z plays a role of an electron transfer intermediate between P680 and cyt b_{559} often in the process of photoinactivation [2]. In case cyt b_{559} was oxidized either chemically or by depletion of the 17- and 23-kDa extrinsic polypeptides, Chl_Z^+ was induced by illumination below 200 K in PS II [33,34]. Trapped Chl_Z^+ EPR signal can be observed at $g \approx 2.0024$ with $\Delta H \approx 10$ G [33] and overlaps on Y_D^+ signal in a Tris-treated PS II with the three extrinsic polypeptides and manganese depleted. Therefore, the radical pair of Y_D^+ and Chl_Z^+, dark-stable radicals at low temperature, are also suitable for the '2 + 1' ESE measurement.

In this paper, we determined the distance between either one of the tyrosines and Q_A^- by using the '2 + 1' pulse sequence ESE method. The radical pair of $Y_D^+Q_A^-$ was trapped in a CN^--treated PS II core complexes by illumination for 8 min, followed by dark adaptation for 3 min at 273 K and freezing into 77 K as in Ref. [17]. The radical pair of $Y_Z^+Q_A^-$ was expected to be trapped by immediate freezing into 77 K after illumination at 253 K for 20 s in the CN^--treated PS II core complexes prepared from spinach. As this trapping method of Y_Z^+ is same as in the Tris-treated PS II membranes [23], there may be a possibility of mixture of Y_Z^+ and Y_D^+ differently from the case obtained by the sample with site-directed mutation of the Y_D residue [17].

By using a proton matrix ENDOR, the trapped radicals were examined to identify which one or two of Q_A^-, Y_D, and Y_Z^+. We also determined the distance between Y_D^+ and Chl_Z^+ by '2 + 1' ESE traces applied to the radical pair induced by illumination at 200 K.

2. Materials and methods

The PS II membranes were prepared from spinach by the method of Kuwabara and Murata [35]. The PS II core complexes were isolated by removing the light-harvesting proteins from PS II membranes, as described in Ref. [36]. Tris-treatments were performed by incubating PS II core complexes on ice under room-light for 30 min in 0.8 M Tris/HCl (pH 8.5). The Tris-treated PS II core complexes were suspended in a solution of 0.2 M sucrose, 20 mM NaCl and Mes/NaOH (pH 5.8 at 20°C) containing 50% glycerol (w/v), stored in liquid N_2, and used for determination of the distance between Y_D^+ and Chl_Z^+. CN^--treatment was performed on the Tris-treated PS II core complexes by the method of Sanakis et al. [32]. The CN^--treated PS II core complexes were finally suspended in solution A (340 mM KCN, 0.34 M sorbitol, 15 mM NaCl, 5 mM $MgCl_2$ and Tricine/NaOH (pH 8.0 at 20°C)) containing 50% glycerol (w/v). To observe the Q_A^- EPR signal only, a part of the CN^--treated PS II core complexes were incubated on ice for 5 min in solution A with addition of 50 mM sodium dithionite, with which Q_A is chemically reduced, and was suspended in the same solution containing 50% glycerol (w/v). Another part of the Tris-treated PS II core complexes were washed two times with solution A without KCN and suspended in the solution containing 50% glycerol (w/v). For comparison with tyrosines trapped in the CN^--treated PS II core complexes by different methods, we observed ENDOR signals of Y_D^+ and Y_Z^+ in this Tris-treated PS II core complexes. All samples were adjusted to give concentrations of 5–6 mg Chl/ml. Illumination of samples was carried out by a 500-W tungsten–halogen lamp through a 10-cm thick water filter.

The '2 + 1' ESE measurements have been performed on a pulsed EPR spectrometer ESP-380 (Bruker) using a pulse sequence shown in Fig. 1. A HP83752B synthesized source (Hewlett Packard) was used as a second m.w. frequency source. The output of this source was fed into a 1-kW TWT amplifier through the second m.w. pulse former unit of ESP 380 (Bruker) microwave bridge giving the second pulse in the pulse sequence shown in Fig. 1. The spectrometer was equipped with a cylindrical dielectric cavity (ER4117DHQ-H, Bruker) and a nitrogen gas flow system (CF935, Oxford Instruments). The measurement temperature was about 80 K and

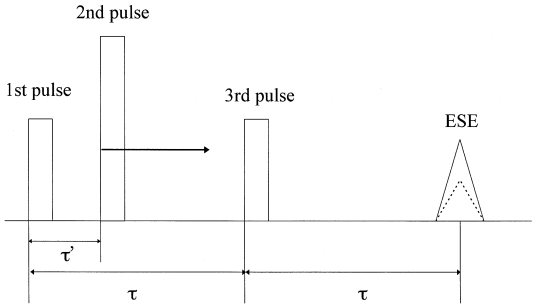

Fig. 1. The pulse sequence of '2+1' ESE method. A primary ESE signal is formed by the first and third m.w. pulses separated by the time interval τ. The amplitude of this signal depends on the second pulse position, τ', as a function of Eq. (1). The durations of microwave pulse used for 1st, 2nd and 3rd were 16, 24, and 16 ns, respectively. The m.w. magnetic field amplitude, H_1, in three pulses was set to provide the spin rotation angles of 30°, 60°, and 30°, respectively.

microwave pulses of 16, 24, and 16 ns durations were used. The m.w. magnetic field amplitude, H1, in the three pulses was set to provide the spin rotation angles of 30, 60, and 30°, respectively.

The ENDOR measurement was carried out on a Bruker ESP300E spectrometer at 105 K using a laboratory-made nitrogen gas flow system. ENDOR signals were observed using modulation of the NMR frequency at 12.5 kHz. The rf power of 250 W from an ENI 3200L power amplifier was supplied to ENDOR coils parallel to the cylindrical axis of TE_{011} mode cavity, and terminated with a 50-Ω dummy load.

The CW-EPR measurement were performed on a Varian E-109 X-band EPR spectrometer at 77 K by using a finger-type dewar inserted in a TE_{102} rectangular cavity to check signals in the trapped state. EPR of Cr^{3+} doped MgO ($g = 1.9800$) attached on the cavity wall was used for references of g values, signal intensities and a microwave power.

3. Theory

In a '2 + 1' ESE method, the spin system is excited by three m.w. pulses as shown in Fig. 1. The first and third pulses, separated by a time interval τ, form a primary ESE signal. The second pulse, separated from the first one by the time interval $\tau'(\tau' \leq \tau)$ changes spin projections of both radical spins relative to the static field direction from $|\alpha>$ to $|\beta>$ and vice versa. If the magnetic dipole interaction between the pairwise-distributed radicals is appreciable, flip of one of the spins changes the local magnetic field at its partner in the pair. As a result, the magnetization after the third pulse cannot be completely refocused at the time 2τ and the amplitude of the primary ESE signal exhibits the dependence on the second pulse position τ' as described in the following expression [23,25]:

$$
\begin{aligned}
V(\tau,\tau') \propto & \left\langle \left(\sin\theta_{\mathrm{A}}^{(1)}\right) C_{\mathrm{A}}^{(2)} S_{\mathrm{A}}^{(3)} \right\rangle_{g(\omega^{\mathrm{A}})} \left\langle 1 - 2S_{\mathrm{B}}^{(3)} \sin^2(D\tau/2) - 2S_{\mathrm{B}}^{(2)} \left\{ \sin^2(D\tau'/2) - S_{\mathrm{B}}^{(3)} \right.\right. \\
& \left.\left. \times \left[\sin^2(D\tau'/2) - \sin^2\left[D(\tau-\tau')/2 \right] + \sin^2(D\tau/2) \right] \right\} \right\rangle_{g(\omega^{\mathrm{B}})} \\
& + \left\langle \left(\sin\theta_{\mathrm{B}}^{(1)}\right) C_{\mathrm{B}}^{(2)} S_{\mathrm{B}}^{(3)} \right\rangle_{g(\omega^{\mathrm{B}})} \left\langle 1 - 2S_{\mathrm{A}}^{(3)} \sin^2(D\tau/2) - 2S_{\mathrm{A}}^{(2)} \left\{ \sin^2(D\tau'/2) - S_{\mathrm{A}}^{(3)} \right.\right. \\
& \left.\left. \times \left[\sin^2(D\tau'/2) - \sin^2\left[D(\tau-\tau')/2 \right] + \sin^2(D\tau/2) \right] \right\} \right\rangle_{g(\omega^{\mathrm{A}})}, \qquad (1)
\end{aligned}
$$

where

$$D = 2\pi D_0 (1 - 3\cos^2\theta). \qquad (2)$$

D is the dipolar interaction constant between spins A and B. $\theta_{\mathrm{i}}^{(j)}$ is the nutation angle of the spin i, either A or

B, induced by the jth pulse. $C_i^{(j)} = \cos^2(\theta_i^{(j)}/2)$, $S_i^{(j)} = \sin^2(\theta_i^{(j)}/2)$, and $\langle \ldots \rangle_{g(\omega i)}$ means the average over the EPR spectrum of the spin i. ω^A and ω^B are the Larmor frequencies of the spins A and B. r is the distance between the spins A and B. θ is the angle between the vector joining the spins A and B and the external magnetic field. In Eq. (1), the most effective terms are given as the following:

$$V(\tau,\tau') \propto \left\langle \left(\sin\theta_A^{(1)}\right) C_A^{(2)} S_A^{(3)} \right\rangle_{g(\omega^A)} \left\langle 1 - 2S_B^{(2)} \sin^2(D\tau'/2) \right\rangle_{g(\omega^B)} + \left\langle \left(\sin\theta_B^{(1)}\right) C_B^{(2)} S_B^{(3)} \right\rangle_{g(\omega^B)} \left\langle 1 - 2S_A^{(2)} \sin^2(D\tau'/2) \right\rangle_{g(\omega^A)}.$$

In a non-oriented system, Eq. (1) is to be averaged over the angle θ:

$$\langle V(\tau,\tau') \rangle \propto \int_0^{\pi} V(\tau,\tau') \sin\theta \, d\theta. \tag{3}$$

From the dipole interaction constant D_0 derived by fitting Eq. (1) to the observed '2 + 1' ESE amplitude, the distance between the spins A and B can be calculated using a point–dipole approximation:

$$D_0 = (g\beta)^2 / hr^3 \tag{4}$$

4. Results and discussion

4.1. Distance between Y_D^+ and Q_A^-

Fig. 2A shows the EPR spectra of overlapped Y_D^+ and Q_A^-, trapped by illumination for 8 min, followed by dark adaptation for 3 min at 273 K and freezing into 77 K in the CN^--treated PS II core complexes. As the

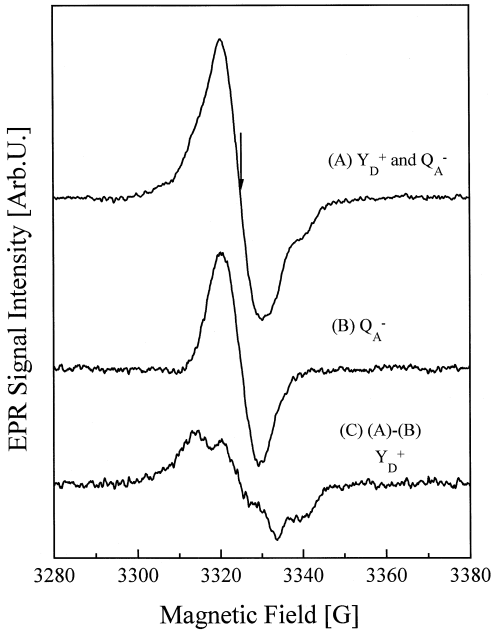

Fig. 2. CW EPR signals of Y_D^+ and Q_A^- in the CN^--treated PS II core complexes observed at 77 K. (A) Overlapped EPR spectra of Y_D^+ and Q_A^-. The arrow indicates the position of $g = 2.0045$, where '2 + 1' ESE traces were observed. Y_D^+ and Q_A^- were trapped by illumination for 8 min followed by dark adaptation for 3 min at 273 K and freezing into 77 K. (B) EPR spectra of Q_A^- (reduced with DTN ($Na_2S_2O_4$)). (C) EPR spectrum of Y_D^+ obtained by a subtraction of (A)–(B). EPR conditions: microwave frequency, 9.34 GHz; microwave power 0.25 μW; field modulation frequency, 100 kHz; field modulation amplitude, 3.2 G.

radical pair $Y_D^+Q_A^-$ in the CN^--treated PS II core complexes was induced in the same way as given by Ref. [17], the trapped tyrosine can be assigned to be Y_D^+. The Q_A^- EPR signal, reduced chemically with sodium dithionite, is shown in Fig. 2B. The Q_A^- EPR signal, observed at $g \cong 2.0045$ with $\Delta H \cong 9$ G, is similar to that observed by Sanakis et al. [32]. Subtraction of the EPR signal of Q_A^- in Fig. 2B from that of Y_D^+ and Q_A^- in Fig. 2A gives a trapped Y_D^+ EPR signal as shown in Fig. 2C. The intensity of Q_A^- signal obtained by double integration of the spectrum in (B) was about 65% of that of Y_D^+ in (C). The EPR signal after subtraction is assigned to tyrosine radicals. However, it is difficult to determine with CW-EPR method whether it is either Y_D^+ or Y_Z^+ or their mixture. To confirm the trapped tyrosine to be Y_D^+, we have carried out the measurement of a proton matrix ENDOR.

First, we observed ENDOR signals of Y_D^+ and Y_Z^+ in the Tris-treated PS II core complexes to see the ENDOR features of Y_D^+ and Y_Z^+. To exclude effects of different pH and solution on the ENDOR spectra, we prepared the Tris-treated PS II core complexes with the solution A without KCN as mentioned above. ENDOR signals were observed at 105 K within the frequency range of 3 MHz centered at the free proton resonance frequency. The magnetic field was fixed at the center of the EPR spectrum ($g = 2.0047$). Fig. 3A shows the ENDOR spectra of overlapped Y_D^+ and Y_Z^+, trapped by immediate freezing into 77 K after illumination for 20 s at 253 K. Fig. 3B shows the Y_D^+ ENDOR signal only, which remained after dark adaptation for 30 min at 273 K. Fig. 3C shows the Y_Z^+ ENDOR signal, obtained by subtraction of the Y_D^+ EDNOR signal in Fig. 3B from the overlapped Y_D^+ and Y_Z^+ ENDOR signal in Fig. 3A. As seen in Fig. 3B, Y_D^+ ENDOR signal is characterized by the peaks A and A′. The value of this peak separation in frequency is shown in Table 1. On the other hand, Y_Z^+ ENDOR signal has no characteristic peaks because of a line-broadening. These ENDOR features of Y_D^+ and Y_Z^+ observed within the frequency range of 3 MHz at 105 K are consistent with those in the previous report [37],

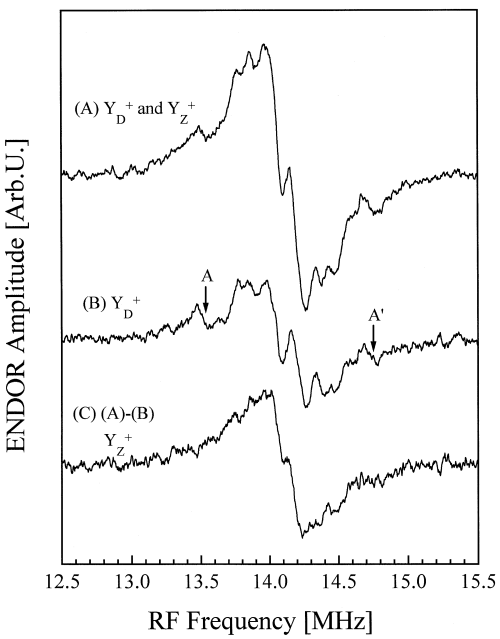

Fig. 3. Proton matrix ENDOR signals of Y_D^+ and Y_Z^+ in the Tris-treated PS II core complexes before CN^--treatment, measured at 105 K. (A) ENDOR spectra of overlapped Y_D^+ and Y_Z^+, trapped by immediate freezing into 77 K after illumination at 253 K for 20 s. (B) ENDOR spectra of Y_D^+ in the Tris-treated PS II core complexes, remained after the dark adaptation of the same sample at 273 K for 30 min after the observation of (A). Y_D^+ is characterized by the peaks AA′. (C) ENDOR spectra of Y_Z^+ in the Tris-treated PS II core complexes, obtained by the subtraction, illuminated (A) − dark-adapted (B). Y_Z^+ has no characteristic peaks due to broadening (see text). ENDOR conditions: Microwave frequency, 9.05 GHz; the fixed microwave power, 0.8 mW; modulation frequency 12.5 kHz; modulation depth, 30 kHz; the magnetic field position; the center of the EPR spectrum ($H_0 = 3305$ G at $g = 2.0047$).

Table 1
ENDOR peak separations (MHz) assigned to Y_D^+ in the Tris-treated, and Y_D^+ and Q_A^- in the CN^--treated PS II core complexes

Peaks	AA′	BB′	CC′	DD′
Sample	Tris	CN^-	CN^-	CN^-
Assignment	Y_D^+	Q_A^-	Q_A^-	Y_D^+
Peak separation	1.20	0.95	1.42	1.18

The absolute error is estimated to be about 50 kHz, while the relative error in frequency separations is estimated to be less than 10 kHz.

where the broadened peaks AA′ of Y_Z^+ ENDOR spectra have been ascribed to a disordered and flexible environment of Y_Z^+ at 105 K. Hence, the proton matrix ENDOR can be used to discriminate Y_D^+ and Y_Z^+ signals.

Fig. 4A shows the ENDOR spectra of the overlapped Y_D^+ and Q_A^-, observed within the frequency range of 3 MHz at 105 K for corresponding EPR shown in Fig. 2A. The magnetic field was fixed at the center of EPR spectrum ($g = 2.0045$) indicated by the arrow there. Fig. 4B shows the Q_A^- ENDOR signal only, after the reduction of the CN^--treated PS II core complexes with sodium dithionite, observed in the same way as in Fig. 4A. In Fig. 4B, Q_A^- ENDOR signal is characterized by peaks BB′ and peaks CC′. The values of these peak separations are shown in Table 1, where the value of 1.42 MHz agrees with that for the matrix proton observed by Rigby et al. [38]. The average value of 1.42 and 0.95 MHz is coincident with the value of the smallest ENDOR separation observed by MacMillan et al. [39]. Fig. 4C shows the Y_D^+ ENDOR signal only, obtained by subtracting Q_A^- ENDOR signal (B) from the overlapped Y_D^+ and Q_A^- ENDOR signal (A). This ENDOR signal has characteristic peaks DD′. The value of this peak separation is also shown in Table 1, which has a similar value as that of peaks AA′ in Fig. 3B, characteristic of Y_D^+ in the Tris-treated PS II core complexes. Furthermore, the ENDOR intensities in the DD′ peak positions have similar magnitudes as those in the peaks

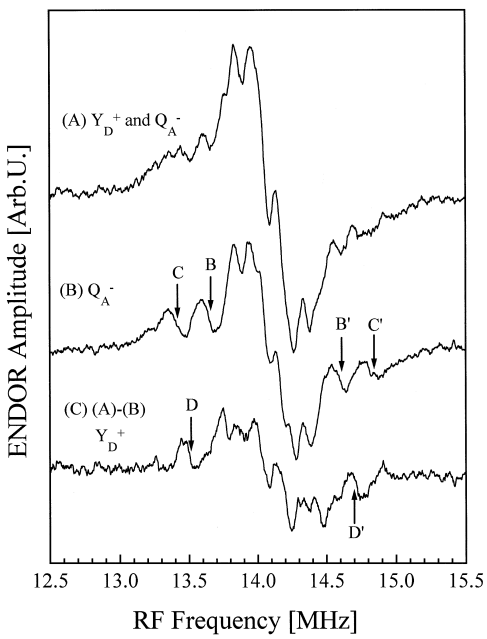

Fig. 4. ENDOR signals of Y_D^+ and Q_A^- in the CN^--treated PS II core complexes, observed at 105 K. (A) Overlapped ENDOR spectra of Y_D^+ and Q_A^-, trapped by illumination for 8 min followed by dark adaptation 3 min at 273 K and freezing into 77 K. (B) ENDOR spectra of Q_A^- (reduced with DTN ($Na_2S_2O_4$)). Q_A^- is characterized by peaks BB′ and CC′. (C) ENDOR spectra of Y_D^+ in the CN^--treated PS II core complexes, obtained by the subtraction illuminated (A) − dark-adapted (B). ENDOR conditions: the same as in Fig. 3.

AA′. Therefore, the radical pair, obtained in the CN^--treated PS II core complexes by illumination for 8 min, followed by dark adaptation for 3 min at 273 K and freezing into 77 K, is assigned to $Y_D^+Q_A^-$ radical pair.

The '2 + 1' ESE experiment was performed at a fixed $\tau = 1080$ ns, with τ' varying from 40 to 1028 ns, where the magnetic field was fixed at the center of EPR spectrum as indicated by the arrow in Fig. 2A. The dependence of the primary ESE amplitude on τ', measured for trapped $Y_D^+Q_A^-$ radical pair in the CN^--treated PS II core complexes, is shown in Fig. 5 by open circles. This time profile reveals about one period of low frequency oscillation and differs remarkably from that obtained for the chemically reduced Q_A^- (filled squares) in the CN^--treated PS II core complexes. Therefore, the difference between these two traces shows an oscillation that could be ascribed to the dipole interaction between Y_D^+ and Q_A^-. To determine the value of the dipole interaction constant D_0 for the $Y_D^+Q_A^-$ radical pair, simulations were carried out using Eqs. (1)–(3) to fit the experimental oscillation pattern. As a result of these simulations, the dipole interaction constant D_0 was found to be 0.89 MHz. From this value, the distance between Y_D^+ and Q_A^- is derived to be 38.8 ± 1.1 Å using Eq. (4). The error of 1.1 Å is smaller than the molecular size of Y_D or Q_A. As a point–dipole approximation, the round value $r \cong 39$ Å can be considered as a good estimate for the distance between Y_D^+ and Q_A^-. As '2 + 1' ESE method can selectively detect the magnetic dipole interaction between a radical pair, the obtained value is most accurate among the values obtained by the other various methods developed so far.

The distance between Y_D and the non-heme Fe(II) was estimated to 37 ± 5 Å from the spin-lattice relaxation time [17]. Considering Q_A is hydrogen-bonded with the histidine coordinating to the non-heme Fe(II) and the non-heme Fe(II) is located at the outer side to the membrane in a purple bacterial reaction center [40], the resulting distance between Y_D–Fe(II) seems to be consistent with the distance obtained here within the experimental error.

We have observed the overlapped EPR spectra of a Y_Z^+-like radical (R^+) and Q_A^-, trapped by immediate freezing of the CN^--treated PS II core complexes into 77 K after illumination for 20 s at 253 K (data not shown). Before illumination, we did not observe any EPR signal at $g = 2.0$ region, which was consistent with the result of Sanakis et al. [32]. The trapped R^+ EPR signal was obtained by subtraction of the EPR signal of Q_A^- from that of R^+ and Q_A^-. By a double integration of the signal, the intensity of R^+ was estimated to be about 80% of that of chemically reduced Q_A^-. In order to prevent the oxidization of Y_D, the illumination time was as short as possible. However, there might be a possibility of mixing of Y_D^+ signal in the R^+ spectra. Although the subtracted EPR signal can be assigned to tyrosine radicals on the basis of its line shape, it is difficult to

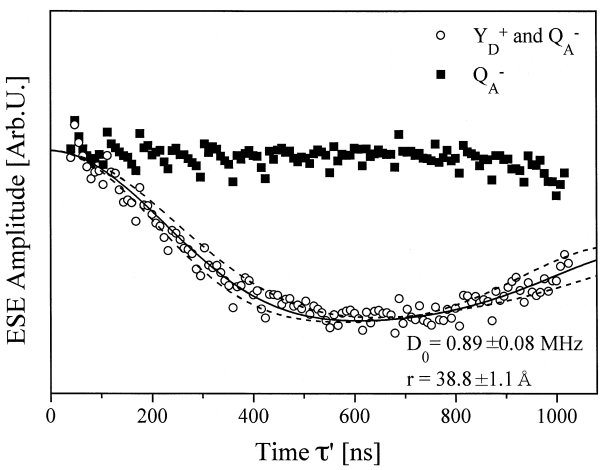

Fig. 5. The '2+1' ESE traces of Y_D^+ and Q_A^- in the CN^--treated PS II core complexes observed at 80 K. Open circles; Y_D^+ and Q_A^-, trapped by illumination for 8 min followed by dark adaptation for 3 min at 273 K and freezing into 77 K. Filled squares: the trace of Q_A^- (reduced with DTN($Na_2S_2O_4$)). Solid line: calculated using Eqs. (1)–(3) for the dipole interaction constant $D_0 = 0.89$ MHz ($D_0 = (g\beta)^2/hr^3$). Dashed line; calculated for frequencies of error limits. All traces are normalized to unity at $\tau' = 0$.

determine whether it includes only Y_Z^+ or a mixture of Y_Z^+ and Y_D^+. Hence, we also examined the same sample by a proton matrix ENDOR.

The ENDOR signal of the overlapped R^+ and Q_A^-, trapped in the CN^--treated PS II core complexes, was observed within the frequency range of 3 MHz at 105 K (data not shown). The ENDOR signal obtained for the trapped radical after subtraction of Q_A^- ENDOR spectra has shown mostly the features assigned to Y_D^+ with some contribution from Y_Z^+-like broadened spectra. Therefore, our trial to trap Y_Z^+ as a major contribution was not successful, probably due to some different kinetic behavior from that in the Tris-treated PS II core complexes. Instead, Y_D^+ has been proved to show two different kinetic behaviors caused by CN^--treatment.

The '2 + 1' ESE experiment was performed in the same way as in Fig. 5. The dependence of the primary ESE amplitude on τ', measured in the CN^--treated PS II core complexes with trapped $R^+Q_A^-$ radical pair, has shown a similar oscillation behavior as shown in Fig. 5. As a result, the dipole interaction constant D_0 between R^+ and Q_A^- was determined to be 0.95 MHz by fitting Eqs. (1)–(3) and the distance between R^+ and Q_A^- is estimated to be 37.8 ± 1.6 Å by Eq. (4).

From the comparison of the distance between Y_D^+ and Q_A^-, the distance between R^+ and Q_A^- is approximately the same within the experimental error, although the distance from R^+ to Q_A^- seems to be slightly shorter than that from Y_D^+. Therefore, we can ascribe the major part of R^+ with a rather first kinetics can be assigned to Y_D^+ with a little shorter distance from Q_A^-. These slight modifications in structure and kinetics might be caused by CN-treatment. To prevent mixing of Chl_Z^+ and other trapped radicals, the trapping method of Y_Z^+ in this work was different from that for the Y_D-less mutant [17], resulting in the failure of the Y_Z^+ trap. Even if the Y_Z^+ trap is successful, other radical species were inevitably trapped in any case. Further studies for systems with more than two radicals will be necessary.

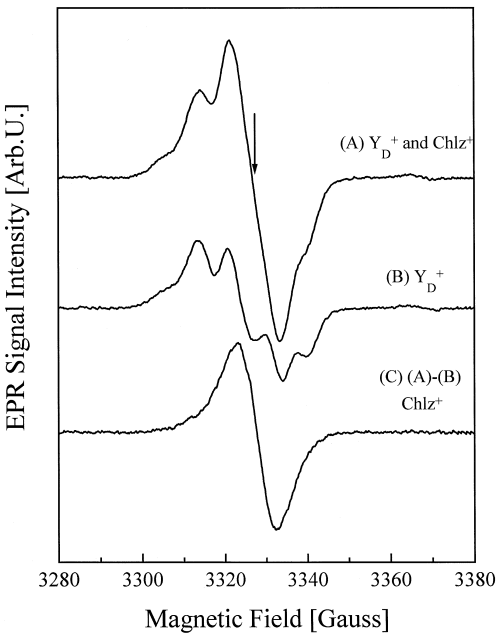

Fig. 6. EPR signals of Y_D^+ and Chl_Z^+ in the Tris-treated PS II core complexes observed at 77 K. (A) Overlapped EPR spectra of Y_D^+ and Chl_Z^+, trapped by freezing into 77 K after illumination at 200 K for 10 min. The arrow shows the position of $g = 2.0024$, where '2+1' ESE traces were observed. (B) EPR spectra of Y_D^+, observed after the dark adaptation of the same sample for 30 min at 273 K. (C) EPR spectrum of Chl_Z^+ obtained by subtraction of (B) from (A). EPR conditions: Microwave frequency, 9.34 GHz; microwave power 0.25 μW; field modulation frequency, 100 kHz; field modulation amplitude, 3.2 G.

4.2. Distance between Y_D^+ and Chl_Z^+

Fig. 6A shows the overlapped EPR spectra of Y_D^+ ($g = 2.0047$) and Chl_Z^+ ($g = 2.0024$), trapped in the Tris-treated PS II membranes by illumination at 200 K for 10 min. Koulougliotis et al. [18] trapped Chl_Z^+ in the CN^--treated PS II membranes by illumination at 77 K. However, Noguchi et al. [34] reported that illumination at 200 K induced the Chl_Z^+ only, while illumination at 80 K induced a mixture of Chl_Z^+ and a radical cation of β-carotene in NH_2OH-treated PS II. In the sample illuminated at 200 K in this work, most of the induced radicals can be assigned to Chl_Z^+ and Q_A^- that is magnetically coupled with non-heme Fe(II). The latter signal had a much wider spectral region and did not contribute the '2 + 1' ESE signal. After the dark adaptation at 273 K for 30 min, only the Y_D^+ EPR signal remained as shown in Fig. 6B. The Chl_Z^+ EPR signal was obtained by subtraction of Y_D^+ EPR signal (B) from the overlapped EPR signals of Y_D^+ and Chl_Z^+ (A) and is shown in Fig. 6C, where $g = 2.0024$ and $\Delta H \cong 10$ G in (C) is different from those of carotenoid radical [41]. By a double integration of the signal, the intensity of Chl_Z^+ was estimated to be about 70% of that of Y_D^+.

The '2 + 1' ESE experiment was performed at the fixed $\tau = 1080$ ns, with τ' varying from 40 to 1032 ns, where the magnetic field was fixed at the center of EPR spectrum indicated by the arrow in Fig. 6A. The dependence of the primary ESE amplitude on τ', observed for the trapped $Y_D^+Chl_Z^+$ radical pair in the Tris-treated PS II core complexes, is shown in Fig. 7 by open circles. This dependence reveals about two periods of low frequency oscillations and differs from that obtained for Y_D^+ (filled squares) in the Tris-treated PS II core complexes corresponding to Fig. 6B after the dark adaptation. Therefore, we could ascribe the oscillations, observed for the trapped radical pair, to the dipole interaction between Y_D^+ and Chl_Z^+. Using Eqs. (1)–(3), the dipole interaction constant D_0 between Y_D^+ and Chl_Z^+ was determined to be 2.05 MHz. From this value of D_0, the distance between Y_D^+ and Chl_Z^+ is estimated to be 29.4 ± 0.5 Å using Eq. (4). As the error of 0.5 Å is much smaller than the size of the molecules of Y_D and Chl_Z, the round value $r \cong 29$ Å can be considered as a correct value for the distance between Y_D^+ and Chl_Z^+.

The location of Chl_Z in PS II was estimated to be 27 Å from the inner and outer thylakoid surfaces, respectively, and to be 39.5 ± 2.5 Å from the non-heme Fe(II) by using the EPR measurement of the spin-lattice relaxation time [18]. In addition to this data, our result, the distance estimated to be 29 Å between Y_D^+ and Chl_Z^+, will give useful information to reveal the electron transfer kinetics related to P680.

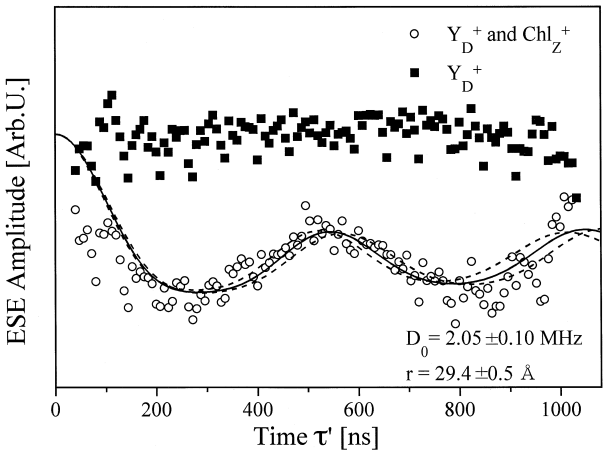

Fig. 7. The '2+1' ESE traces of Y_D^+ and Chl_Z^+ in the Tris-treated PS II core complexes observed at 80 K. Open circles; Y_D^+ and Chl_Z^+, trapped by freezing into 77 K after illumination at 200 K for 10 min. Filled squares; Y_D^+, observed after dark-adaptation of the same sample at 273 K for 30 min. Solid line; calculated using Eqs. (1)–(3) for the dipole interaction constant $D_0 = 2.05$ MHz ($D_0 = (g\beta)^2/hr^3$). Dashed line; calculated for frequencies of error limits. All traces are normalized to unity at $\tau' = 0$.

5. Conclusion

We detected the dipole interaction between selected radical pairs, $Y_D^+Q_A^-$ and $Y_D^+Chl_Z^+$, in photosystem II by using the '2 + 1' pulse sequence ESE method. The $Y_D^+Q_A^-$ radical pair was trapped at 77 K by freezing after illumination for 8 min followed by dark adaptation for 3 min at 273 K in the CN^--treated PS II core complexes. In order to trap the $Y_Z^+Q_A^-$ radical pair, a short period illumination for 20 s of the same sample was also carried out at 253 K and freezed at 77 K immediately after illumination. By using a proton matrix ENDOR, both tyrosines, trapped by different methods, are confirmed to be Y_D^+. The Y_D^+ radical with a fast decay kinetics may be ascribed to the structural irregularity caused by the CN-treatment. We could trap $Y_D^+Chl_Z^+$ radical pair by illumination of the Tris-treated PS II core complexes at 200 K. Using Eqs. (1)–(4) for the ESE oscillation induced by dipolar interaction between a radical pair, the distances of Y_D^+–Q_A^- and Y_D^+–Chl_Z^+ are determined to be 38.8 ± 1.1 Å and 29.4 ± 0.5 Å, respectively. The obtained values of distance are most accurate among the values obtained by other various methods.

Acknowledgements

This work was supported by grant-in-aid for General Research (No.06452073) from the Ministry of Education, Science and Culture of Japan and a special research fund from Kwansei Gakuin University to A.K. Kind advises to this work are indebted to Dr. H. Mino in Photosynthetic Research Laboratory of the Institute of Physical and Chemical Research (RIKEN), Wako 251-01, Japan.

References

[1] R.J. Debus, Biochim. Biophys. Acta 1102 (1992) 269–352.
[2] A.-F. Miller, G.W. Brudvig, Biochim. Biophys. Acta 1056 (1991) 1–18.
[3] T. Inui, A. Kawamori, G. Kuroda, T. Ono, Y. Inoue, Biochim. Biophys. Acta 973 (1989) 147–152.
[4] C.W. Hoganson, G.T. Babcock, Biochemistry 27 (1988) 5848–5855.
[5] J.P. Dekker, H.J. van Gorkom, M. Brok, L. Ouwehand, Biochim. Biophys. Acta 764 (1984) 301–309.
[6] B. Svensson, I. Vass, E. Cedergren, S. Styring, EMBO J. 7 (1990) 2051–2059.
[7] S.V. Ruffle, D. Donnelly, T.L. Blundell, J.H.A. Nugent, Photosyn. Res. 34 (1992) 287–300.
[8] J. Deisenhofer, O. Epp, K. Miki, R. Huber, H. Michel, Nature 318 (1985) 618–624.
[9] J.P. Allen, G. Feher, T.O. Yeates, H. Komiya, D.C. Rees, Proc. Natl. Acad. Sci. U.S.A. 84 (1987) 5730–5734.
[10] A. Trebst, Z. Naturforsch. 41c (1986) 240–245.
[11] H. Michel, J. Deisenhofer, Biochemistry 27 (1988) 1–7.
[12] B. Svensson, I. Vass, S. Styring, Z. Naturforsch. 46c (1991) 62–73.
[13] B. Svensson, C. Etchebest, P. Tuffery, P. van Kan, J. Smith, S. Styring, Biochemistry 35 (1996) 14486–14502.
[14] Y. Kodera, K. Takura, A. Kawamori, Biochim. Biophys. Acta 1101 (1992) 23–32.
[15] D.J. Hirsh, G.W. Brudvig, J. Phys. Chem. 97 (1993) 13216–13222.
[16] J.B. Innes, G.W. Brudvig, Biochemistry 28 (1989) 1116–1125.
[17] D. Koulougliotis, X.-S. Tang, B.A. Diner, G.W. Brudvig, Biochemistry 34 (1995) 2850–2856.
[18] D. Koulougliotis, J.B. Innes, G.W. Brudvig, Biochemistry 33 (1994) 11814–11822.
[19] Y. Kodera, H. Hara, A.V. Astashkin, A. Kawamori, T. Ono, Biochim. Biophys. Acta 1232 (1995) 43–51.
[20] C.W. Hogansson, N. Lydakis-Simantiris, X.-S. Tang, C. Tommos, K. Warncke, G.T. Babcock, B.A. Diner, J. McCracken, S. Styring, Photosyn. Res. 46 (1995) 177–184.
[21] M.L. Gilchrist Jr., J.A. Ball, D.W. Randall, R.D. Britt, Proc. Natl. Acad. Sci. U.S.A. 92 (1995) 9545–9549.
[22] H. Hara, A. Kawamori, A.V. Astashkin, T. Ono, Biochim. Biophys. Acta 1276 (1996) 140–146.
[23] A.V. Astashkin, Y. Kodera, A. Kawamori, Biochim. Biophys. Acta 1187 (1994) 89–93.
[24] V.V. Kurshev, A.M. Raitsimring, Yu.D. Tsvetkov, J. Magn. Reson. 81 (1989) 441–454.
[25] V.V. Kurshev, A.M. Raitsimring, T. Ichikawa, J. Phys. Chem. 95 (1991) 3564–3568.
[26] K. Warncke, G.T. Babcock, J. McCracken, J. Am. Chem. Soc. 116 (1994) 7332–7340.

[27] S.E.J. Rigby, J.H.A. Nugent, P.J. O'Malley, Biochemistry 33 (1994) 1734–1742.
[28] C. Tommos, X.-S. Tang, K. Warncke, C.W. Hoganson, S. Styring, J. McCracken, B.A. Diner, G.T. Babcock, J. Am. Chem. Soc. 117 (1995) 10325–10335.
[29] X.-S. Tang, M. Zheng, D.A. Chisholm, G.C. Dismukes, B.A. Diner, Biochemistry 35 (1996) 1475–1484.
[30] H. Mino, A.V. Astashkin, A. Kawamori, Spectrochim. Acta 53 (1997) 1465–1483, Part A.
[31] A.W. Rutherford, J.L. Zimmermann, Biochim. Biophys. Acta 767 (1984) 168–175.
[32] Y. Sanakis, V. Petrouleas, B.A. Diner, Biochemistry 33 (1994) 9922–9928.
[33] L.K. Thompson, G.W. Brudvig, Biochemistry 27 (1988) 6653–6658.
[34] T. Noguchi, T. Mitsuoka, Y. Inoue, FEBS Lett. 356 (1994) 179–182.
[35] T. Kuwabara, N. Murata, Plant Cell Physiol. 23 (1982) 533–539.
[36] D.F. Ghanotakis, D.M. Demetriou, C.F. Yocum, Biochim. Biophys. Acta 891 (1987) 15–21.
[37] H. Mino, A. Kawamori, Biochim. Biophys. Acta 1185 (1994) 213–220.
[38] S.E.J. Rigby, P. Heathcote, M.C.W. Evans, J.H.A. Nugent, Biochemistry 34 (1995) 12075–12081.
[39] F. MacMillan, F. Lendzian, G. Renger, W. Lubitz, Biochemistry 34 (1995) 8144–8156.
[40] J.P. Allen, G. Feher, T.O. Yeates, H. Komiya, D.C. Rees, Proc. Natl. Acad. Sci. U.S.A. 85 (1988) 8487–8491.
[41] Y. Wu, L. Piekara-Sady, L.D. Kispert, Chem. Phys. Lett. 180 (1991) 573–577.